Accepted Manuscript

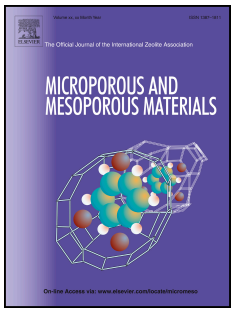

Tunable porous boron nitride: Investigating its formation and its application for gas adsorption

Sofia Marchesini, Anna Regoutz, David Payne, Camille Petit

PII: S1387-1811(17)30051-3

DOI: 10.1016/j.micromeso.2017.02.010

Reference: MICMAT 8120

To appear in: *Microporous and Mesoporous Materials*

Received Date: 13 July 2016

Revised Date: 15 January 2017

Accepted Date: 1 February 2017

Please cite this article as: S. Marchesini, A. Regoutz, D. Payne, C. Petit, Tunable porous boron nitride: Investigating its formation and its application for gas adsorption, *Microporous and Mesoporous Materials* (2017), doi: 10.1016/j.micromeso.2017.02.010.

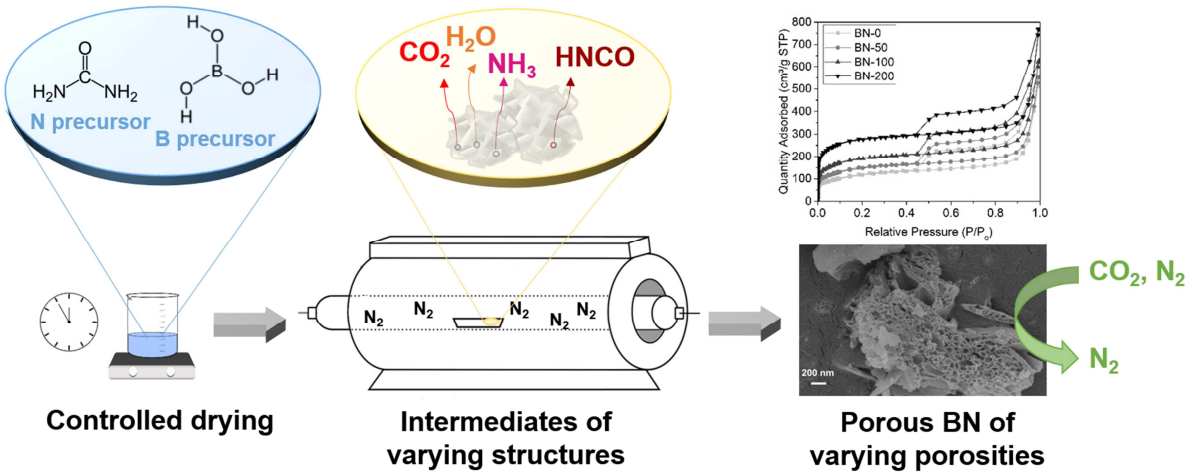

Tunable porous boron nitride: investigating its formation and its application for gas adsorption

Sofia Marchesini,[a] *Anna Regoutz,*[b] *David Payne*[b] *and Camille Petit*[a,*]

[a] Department of Chemical Engineering, Imperial College London, South Kensington Campus, London SW7 2AZ, UK

[b] Department of Materials, Imperial College London, South Kensington Campus, London SW7 2AZ, UK

Abstract

Boron nitride (BN) has applications in a number of areas: it can be used as lubricant, as insulating thermoconductive filler or UV-light emitter. BN can also capture large amounts of hydrocarbons and gaseous molecules, provided that it exhibits a porous structure. This porous structure also enables its application as a drug-delivery nanocarrier. Little if anything is known on controlling the porosity of BN, even though it has tremendous implications in terms of adsorption performance and drug delivery properties. To address

* Corresponding Author: Camille Petit, camille.petit@imperial.ac.uk

this aspect, we provide for the first time an in-depth investigation of the effects of the synthesis conditions on the formation of porous BN. The material was also tested for CO_2 capture. We found that the intermediate preparation is of paramount importance and can in fact be used to tune the porosity of BN. Owing to a combination of spectroscopic and thermal analyses, we attributed this phenomenon to the variation of the thermal decomposition pattern of the intermediates. The most microporous BN produced was able to capture CO_2 while not retaining N_2. Overall, this study opens the route for the design of well-controlled porous BN structures to be applied as adsorbents and drug-delivery carriers.

Keywords: boron nitride, adsorption, X-ray photoelectron spectroscopy, porosity, CO_2 capture

1. INTRODUCTION

Hexagonal boron nitride (h-BN) is a 2D-layered material composed of boron and nitrogen atoms arranged in a honeycomb-like structure. It exhibits high thermal, chemical and mechanical stability, and a 'richer' chemistry compared to carbon-based materials, due to the polarity of B-N bonds. Boron nitride can be obtained with high surface area either in the form of an amorphous porous material – somewhat similar to activated carbon – or in the form of nanosheets, obtained by isolating single- or few-layer sheets of h-BN [1-3]. The former type of BN represents an attractive material for drug delivery, especially considering its non-toxicity. The porous feature of BN is also of interest in the field of adsorption. Porous BN can be seen as a new class of highly robust adsorbents that is complementary to carbonaceous materials, owing to the high thermal and chemical stability of BN. Recent studies have reported the use of porous BN for gas phase and liquid phase adsorption. The focus has mostly been on CO_2 capture [4-6], H_2 storage [7-10], pollutants removal from air [11, 12], water pollutants removal [7, 12-22] and oil adsorption [15, 21, 22]. For instance, recent work by Nag et al. [5] reported the synthesis of boron nitride with a CO_2 adsorption capacity of up to 32 wt. % at 195 K and 0.85 P/P_o. Furthermore, it was demonstrated by Zhao et al. that boron nitride 3D foam could adsorb between 70 and 190 times its weight in organic pollutants and oils [22].

Porous BN can be produced in a rather straightforward manner via bottom-up synthesis approaches. A number of these approaches have been developed and can be broadly divided into three classes: "chemical blowing" technique, template-based methods and template-free methods. Chemical blowing consists of heating ammonia borane up to

1400 °C under an inert atmosphere. While relatively easy to implement, this technique relies on the use of an expensive precursor (ammonia borane) and results in a low surface area material (< 150 m^2/g) [23, 24]. The second class of synthesis method – templating method – uses a sacrificial material to control the porosity of the resulting BN. Some examples of templates employed include mesoporous silica, carbonaceous materials and zeolites [25-27]. Various organic compounds have also been mixed with boron and nitrogen precursors and used as structure-directing agents to produce porous BN, such as for instance cetyl-trimethylammonium bromide [28], or the triblock copolymer (P123) [12]. In general, it is found that the use of inorganic templates leads to materials with lower surface areas compared to organic ones (300-600 m^2/g vs 800-2000 m^2/g). To avoid the use of a template, and hence reduce the number of synthesis steps and associated cost, template-free methods have been developed. Overall, solid nitrogen and boron precursors – typically melamine/urea and boron oxide/boric acid – are mixed and heat treated (500-2000 $^{\circ}$C) under an inert atmosphere [5, 7-9, 11, 17, 18, 29-32]. In some cases though, ammonia gas is used as the nitrogen precursor. Following this approach, materials with surface areas up to about 1,700 m^2/g have been obtained [7]. Despite the straightforward nature of this method and its potential for scale-up, little is known on the effects of the synthesis parameters (i.e. precursor ratios, temperature, atmosphere, etc…) on the physical and chemical properties of the resulting materials. Nevertheless, if one wants to employ porous BN for specific adsorption applications or as catalyst support, the properties of the materials must be carefully controlled as they can directly influence the adsorption performance and the deposition of catalyst particles. In fact, some preliminary studies indicate that synthesis conditions probably have a significant impact on the structural and

chemical properties of porous BN. For instance, Nag and coworkers showed that varying the initial ratio of precursors prior to heating, led to a three-fold increase in the surface areas of the resulting BN [5]. It is also interesting to note that in most studies, the nitrogen and boron precursors are first mixed in a solvent – often methanol or water – prior to the heat treatment leading to BN formation. While this step was employed in most studies, no justification for it was given until a recent study by Wu and coworkers provided a greater insight on the impact of this step on BN formation [33]. It was demonstrated that the specific surface area of BN could be tailored by recrystallizing a mixture of urea and boric acid from solvents with different boiling points. The different boiling points of the solvents had an effect on the crystalline structure of the intermediates and subsequently on their decomposition during heat treatment and hence on the structure of the resulting porous BN. In summary, the status of research on the formation (and production) of porous BN does not provide the necessary understanding to tune the material's properties for given applications, particularly adsorption.

In this study, we aim to provide an in-depth investigation of the synthesis conditions on the formation of porous BN. This is meant to unlock the potential of a new class of robust adsorbents. To do so, we employed a template-free method using urea and boric acid as the precursors. Before the heat treatment, the chemicals were mixed in water and dried for various durations, resulting in the formation of a solid intermediate. This was done to investigate the impact of the pre-heat treatment step. Both the porous BN samples and the intermediate samples were characterized by spectroscopic (FTIR, XPS), crystallographic (XRD), imaging (SEM, TEM) and analytical techniques (N_2 sorption, TGA) in order to

provide a complete picture of the structure, morphology and chemistry of the samples and relate these to synthesis conditions. Given the high porosity and particularly high microporosity of the BN samples obtained, and taking into account the presence of N-groups, preliminary CO_2 adsorption tests were conducted.

2. EXPERIMENTAL

2.1. Material synthesis

In a typical experiment, urea (9 g, molecular biology grade, Sigma-Aldrich) and boric acid (1.85 g, ACS reagent, Sigma-Aldrich) were dissolved in deionized water (450 mL) at 65 °C, and the water was then allowed to completely evaporate at that temperature. The white powder obtained – referred to as the intermediate – was further dried in the oven at 65 °C for different lengths of time (0 h, 50 h, 100 h, 200 h). The resulting intermediate samples are named: INT- X. “INT” stand for intermediate and “X” is the drying time in hours after the complete evaporation of the water. The intermediates were ground and loaded in an alumina boat crucible and then heated in a tubular furnace under nitrogen atmosphere (flow of 50 mL min^{-1}) from room temperature to 1050 °C at a rate of 10 °C min^{-1}. This temperature was maintained for 3.5 h. The samples were allowed to cool to ambient temperature (natural cooling rate) while maintaining the same nitrogen flow. At the end of the synthesis, a white powder (porous BN) was obtained. The samples are referred to as BN-X, in the same way as for the intermediates, with “BN” referring to porous BN and “X” to the drying time of the intermediate. For comparison, porous BN was

also synthesized using a physical mixture of urea and boric acid in the same molar ratio. In this case, urea and boric acid were physically mixed (molar ratio of 5, as for the other samples), ground together, placed in a ceramic boat and then subjected to the same heat treatment as the intermediate samples. The resulting BN sample is referred to as BN-phys mix. It must be noted that about 300 mg of sample was obtained for each synthesis.

2.2. Materials characterization

2.2.1. Chemical properties: The intermediates and resulting porous BN samples were characterized by Fourier Transform Infrared (FT-IR) spectroscopy. The samples were first ground in an agate mortar and spectra were collected in the range of 600-4000 cm^{-1} using a Perkin-Elmer Spectrum 100 Spectrometer equipped with an attenuated total reflectance (ATR) accessory. X-Ray Photoelectron Spectroscopy (XPS) was performed using a Thermo Scientific K-Alpha^{+} X-ray Photoelectron Spectrometer equipped with a MXR3 Al Kα monochromated X-ray source (hν = 1486.6 eV). X-ray gun power was set to 72 W (6 mA and 12 kV). Survey scans were acquired using 200 eV pass energy, 0.5 eV step size and 100 milliseconds (50 ms x 2 scans) dwell times. All high resolution spectra (B 1*s*, N 1*s*, C 1*s*, and O 1*s*) were acquired using 20 eV pass energy, 0.1 eV step size. The samples were ground and mounted on the XPS sample holder using conductive carbon tape. Thermo Avantage was used for analysis of the XPS data. The XPS spectra were shifted to align the peak for adventitious carbon (C-C) at 285.0 eV. A thermogravimetric analyser coupled with a mass spectrometer (TGA-MS) was used to study the decomposition of the intermediates (TGA: Mettler Toledo LMX 1, MS: Hiden Analaytical HPR 20 Evolved). In a typical run,

the samples were placed in an alumina crucible and heated from 30 to 1050 ºC (10 ºC min^{-1} ramp rate), with a 30 minute holding step at 100 ºC.

2.2.2. Structural properties and morphology: Powder X-ray diffraction (XRD) was performed using an X-ray diffractometer (PANalytical X'Pert PRO) in reflection mode. The operating conditions included an anode voltage of 40 kV and an emission current of 40 mA using a monochromatic Cu Kα radiation (λ = 1.54178 Å). The XRD detector used was X'Celerator (silicon strip detector). Nitrogen sorption isotherms were measured using a porosity analyser (Micromeritics 3Flex) at -196 °C. Prior to the measurement, the samples were degassed overnight at 120 °C at roughly 0.2 mbar pressure. They were finally degassed in-situ on the porosity analyser for 4 h down to around 0.0030 mbar. The equivalent surface areas of the samples were calculated using the Brunauer-Emmett-Teller (BET) method. The total volume of pores was calculated from the volume of N_2 adsorbed at P/P_0 = 0.97. The micropore volume was determined using the Dubinin-Radushkevich method. The morphology of the samples was evaluated using a Scanning Electron Microscope (SEM, Leo Gemini 1525) in secondary electron mode at 5 kV as well as a high-resolution Transmission Electron Microscopy (TEM, Jeol 2100FX).

2.2.3. Gas sorption analyses: CO_2 sorption was performed on a Micromeritics 3Flex sorption analyzer at 25 °C, using a waterbath to control the temperature. The samples (~ 100 mg) were degassed overnight at 120 °C at roughly 0.2 mbar pressure and further degassed *in-situ* for 4 hours down to around 0.0030 mbar, before the start of the analysis. N_2 and CO_2 sorption were also performed on a TGA analyser at 25 °C after degassing the

sample at 120 °C in the vacuum oven overnight and additionally degassing the sample *in-situ* at 120 °C for 1 h under N_2 atmosphere.

3. RESULTS AND DISCUSSION

First, the chemical features of the porous BN obtained from the different intermediates were analyzed using FTIR spectroscopy. As seen in **Fig. 1**, all spectra exhibited the two main characteristic bands of boron nitride at ~ 1360 cm^{-1} (B-N in-plane transverse stretching mode) and at 800 cm^{-1} (B-N-B out-of-plane bending mode) [34]. No major chemical differences could be observed between the samples. To gain further insight into the chemistry of the materials, XPS was used and the results are reported in **Fig. 2**. It must be noted that only the peak fit spectra of the BN-phys mix sample are shown as all samples exhibited similar chemical features. However, the relative atomic percentages are reported for all samples in the same Figure (bar plot). The presence of BN is confirmed by the main contributions to the B 1*s* and N 1*s* core level at binding energies of 191.0 eV and 398.5 eV, respectively. These values agreed well with those reported in the literature of 190.5-191.1 eV for B 1*s* and 397.6-398.7 eV for N 1*s* for boron nitride [35, 36]. The B 1*s* and N 1*s* spectra of porous BN also exhibited shake-up satellite peaks, which confirm the presence of sp^2- hybridised BN in the hexagonal phase, as previously reported [37-39]. In addition to BN, XPS revealed the presence of between 10 and 13 at.% ± 1 at.% of oxygen impurities (**Fig. 2**). The carbon content was very low (between 2 and 4 at.% ± 1 at.%) and can be attributed to adventitious carbon present as surface impurity, it was therefore not included in the atomic percentage bar plot in **Fig. 2**. It is important to note that many prior studies did not report elemental analysis of porous boron nitride, however it is believed that

the samples discussed probably contained oxygen given the similar synthetic approach. The presence of O groups modifies the chemistry and therefore adsorptive properties of a material and it is therefore important to take it into account. The elemental ratios remained relatively stable between the different samples with a higher boron content (~ 52 at.%) compared to nitrogen (~37 at.%). The higher boron content was probably due to the higher volatility of the nitrogen precursor. Based on the peak fit, the oxygen impurities were assigned to boronoxynitride BO_xN_y species, with a binding energy of 192.5 eV, which concurs with the previous findings [40]. The boronoxynitride was probably part of the crystal lattice within the BN layers or at the edges of these layers. It must be noted that no contaminants other than C and O were observed in the samples (Supplementary **Fig. S2**). The three main conclusions of the XPS analyses are that: (i) boron nitride was formed, (ii) O impurities were present in relatively significant quantities, and (iii) the chemical features of the various samples were very similar, as supported by FT-IR spectroscopy (**Fig. 1**).

Taking into account their very similar chemistry, the physical and structural properties of the samples were then analysed in order to identify any potential differences indicating an effect of the synthesis parameters on the resulting materials. The crystallinity of the porous BN samples obtained from various intermediates was analyzed using XRD. As shown in **Fig. 3**, the XRD patterns displayed the (002) and (100) peaks corresponding to hexagonal BN (JCPDS card no. 34-0421) [41]. The absence of the (004) peak is due to its typically very low intensity compared to the (002) and (100). The d-spacing for the (002) plane (**Table 1**), corresponding to the distance between the different layers, was larger than that reported in the literature for bulk h-BN (3.3 Å) [2] and slightly increased with the

intermediates' drying time from 3.51 Å for BN-0 to 3.60 Å for BN-200 and BN phys mix. The larger d-spacing was probably related to the non-planar texture of the BN layers owing to the presence of defects (e.g. O groups as indicated by XPS study above). The presence of trapped molecules like water was however ruled out due to the high temperature used to produce porous BN and the hydrophobic nature of boron nitride. The XRD peaks were very broad and exhibited low intensities, indicating the presence of a turbostratic structure, a structure that is half way between hexagonal and amorphous [30]. It is interesting to notice that the crystallinity slightly increased in samples prepared with intermediates dried for a shorter time.

While the chemical features did not visibly change with the change in the intermediate drying time, the XRD patterns point to some structural variations. Further analyses were therefore conducted to get a greater insight. To characterize the nano/microscale features of the samples, their porosity was analyzed using nitrogen sorption at -196 °C. The resulting isotherms exhibited a type I/IV isotherm indicating the presence of both micropores and mesopores (**Fig. 5)**. Type H3/H4 hysteresis were also visible which is typical for slit shape pores. **Table 1** summarizes the textural parameters of the porous BN samples synthesized from various intermediates. It can be observed that the BET equivalent surface area and volume of pores noticeably increased for samples prepared from intermediates dried for longer times going up to 1016 m^2/g and 0.869 cm^3/g, respectively. It is also interesting to notice that the proportion of micropores increased with the drying time. As seen in **Table 1**, the sample prepared from a physical mixture of precursors exhibited a porosity similar to that of BN-200.

Since it was clear from the above measurements that the intermediate drying time had an effect on the microscale structure of the resulting porous BN, we then investigated whether this was also the case at the macroscale. The morphology of the porous BN samples was characterized using high resolution SEM. As shown in **Fig. 5**, the samples exhibited two main features: a flake-like morphology (**Fig. 5A**) and a more porous structure (**Fig. 5B**). These features were visible on all samples. In addition, high-resolution TEM was used and the images (**Fig. 6**) highlighted the typical disordered turbostratic structure as supported by the XRD patterns. Again no major differences between the various samples could be observed.

In order to understand why the drying time of the intermediate affected the porosity of BN samples, the chemical and physical features of the different intermediates were analyzed. The FTIR spectra of the intermediates were compared to those of urea and boric acid (Supplementary **Fig. S1**). No additional bands other than that from urea and boric acid could be observed, indicating no major change in the chemical composition and therefore most probably no chemical reaction between the two precursors. This is in agreement with the findings of Wu and coworkers [33]. Only weak interactions might have been present. To understand whether the intermediates formed only a physical mixture or involved interactions between boric acid and urea (as would be expected), XPS analysis was performed on two intermediates (INT-0 and INT-200), as well as on the physical mixture of urea and boric acid (INT-phys mix). The results are presented in **Fig. 7**. The spectra were normalized to the O 1*s* peak. As shown, the peaks appeared at similar position and exhibited similar shape regardless of the sample, indicating that there was no significant

chemical difference between the different intermediates including the physical mixture. This observation suggested the absence of strong bonds being formed between the precursors which, albeit surprising, is in good agreement with the FTIR results (Supplementary **Fig. S1**). The peak-fitted core level XPS spectra for a typical intermediate sample were also reported in **Fig. S3**. Observing the B 1*s* spectra of the intermediates in **Fig. 7** and **Fig. S3**, the main peak, (Figure 7, B 1*s*, peak [2]), at binding energies of 192.7-192.9 eV, is in good agreement with the literature value for boric acid [40]. Urea was also present as indicated by the main peak (**Fig. 7**, N 1*s*, peak [2]) at binding energies of 400.0-400.2 eV, which correspond to the experimentally measured value for urea (400.0 eV, data not shown here). The N 1*s* and B 1*s* spectra also exhibited additional peaks (peak [1]) probably belonging to impurities present in the urea and boric acid precursor, respectively. These impurities have not been identified but appeared in the physical mixture as well as the intermediates, indicating that no reaction happened during the dissolution step. The O 1*s* spectra showed the presence of two peaks, one associated with urea (peak [2]) in agreement with the experimentally measured value (not shown) and the other was assigned to boric acid (peak [1]). The C 1*s* spectra exhibited 3 peaks, peak [1] corresponding to the carbon in urea, in good agreement with the experimentally measured value, some C impurity not yet identified, peak [2], and adventitious carbon (C-C) (peak [3]). The elemental ratios varied between samples, as indicated by differences in peak intensities, but did not exhibit any trend or at least no justifiable trend at this stage of the study (this was also observed on other intermediate samples).

XRD was used to characterize the intermediates (the ones before any heat treatment at 250 °C, INT-X) (**Fig. 8**). No new peaks other than those from urea and boric acid were observed ruling out the formation of a new crystalline structure. Owing to the absence of a dissolution step, the physical mixture exhibited a different crystalline structure compared to that of the intermediate samples (higher relative intensity of (110)/(101) reflections for urea). The peak related to boric acid was visible on the XRD pattern of the physical mixture while this was not the case for the intermediate samples. This is attributed to the fact that boric acid molecules were better mixed in the latter samples.

The visible difference in crystallinity (difference in relative intensities) between the various intermediates (and the physical mixture) may have had an impact on the thermal decomposition profile of the samples[42], which in turn could have influenced the morphology of the resulting materials. To investigate this aspect, the intermediates as well as the physical mixture were analyzed using TGA-MS. The TG curves are presented in **Fig. 9** while the mass spectra of various species released during decomposition are plotted in **Fig. 10**. The most noticeable feature on **Fig. 9** was the fact that between 160 ºC and 250 ºC the intermediates dried for longer exhibited a lower mass loss. This could be due to the formation of a larger quantity of a thermostable BN precursor for samples dried for longer. As seen in **Fig. 10**, two major weight losses were observed that coincide with the release of four different gases, namely ammonia, carbon dioxide, isocyanic acid and water. Intermediates dried for longer started decomposing at lower temperatures. Moreover, the physical mixture, despite showing a similar TGA decomposition curve to INT-0, exhibited an additional peak in **Fig. 10** (for ammonia and carbon dioxide) at lower temperatures (<

200 °C) compared to the intermediates. Clearly, the decomposition patterns of the samples were different. More specifically, the intermediates dried for longer started decomposing at lower temperatures and hence it was hypothesized that a thermostable BN precursor started forming in larger quantities compared to the intermediates dried for a shorter duration. This in turn probably led to the formation of BN with a higher porosity. This is because in the temperature range 100 °C – 250 °C, more gases were released from the decomposition of urea and boric acid. These gases acted as porogens during the formation of the more stable BN precursor. This BN precursor exhibiting enhanced porosity led to the formation of BN with enhanced porosity as well. It must be noted that gases were released at relatively low temperature during the decomposition of the physical mixture. Hence, these must have acted as porogens as well and explain the high porosity observed for BN-phys mix sample despite the different crystalline structure of the physical mixture compared to that of the intermediate samples dried for a long time.

In order to confirm whether a BN precursor was formed during the heat treatment of the intermediates below 250 °C and to gain insight of its structure, INT-0 and INT-100 were heated in a tubular furnace up to 250 °C (10 °C/min) under nitrogen gas flow, maintaining the same conditions previously used for the synthesis of BN. Both intermediates, as well as the products obtained at 250 °C, referred to as INT-0-250 and INT-100-250, were analyzed using XPS. It must be noted that the intermediates were heat-treated up to 250 °C and then cooled and analyzed in order to study the formation of a BN precursor. At 250 °C, the intermediates are expected to be mostly in the form of a melt, with some amorphous BN precursor and some boronoxynitride. **Figure 11** reports INT-0 before heat treatment, when

heated to 250 °C (INT-0-250) and also to 1050 °C (BN-0) in order to form porous BN. INT-0 contained a mixture of urea and boric acid, plus a small amount of impurities not yet identified. One can notice that changes started to appear for INT-0 as the sample was heated at 250 °C. In particular, there was the appearance of two new peaks related to the formation of the B-N bond: ~398.5 eV (B 1*s*) and ~191.0 eV (N 1*s*). The formation of h-BN was also confirmed by the presence of two broad peaks at higher binding energies in the B 1*s* and N 1*s* core level spectra, which are due to the π-π^* transition only present in the hexagonal form of BN [38]. It must be noted that the presence of h-BN is most probably localized with islands of h-BN separated by more amorphous parts (as suggested from the TEM images). The B 1*s* peak for boric acid at 192.7 eV in INT-0 shifted to lower binding energy (192.3 eV) when the sample was heated at 250 °C (INT-0-250), indicating that some OH groups were probably substituted by less electronegative NH_2 groups, as previously reported by Gouin et al. in a nitridation of boric acid under ammonia atmosphere [40]. Boronoxynitride was still present in the final BN-0 product (B 1*s*), heated at 1050 °C, however it exhibited a lower nitrogen content. The N 1*s* peak for urea at 400.1 eV in INT-0 also shifted to lower binding energy (399.5 eV) when heated to 250 °C. This peak was assigned to a boronoxynitride and NH_2 species reacting with boric acid. The C 1*s* and O 1*s* core level spectra for INT-0, INT-0-250 and BN-0 are reported in supporting information (Supplementary **Fig. S4**). It is worth noting that INT-100 is not reported here as it exhibited similar chemical features to INT-0. Overall, XPS confirmed that BN (along with boronoxynitride) started forming at temperatures as low as 250 °C. The presence of BN was further confirmed by FTIR spectroscopy (**Fig. S5**). The spectrum of INT-0-250 shows the typical h-BN bands at 775 and 1390 cm^{-1}, as previously reported by Gouin et al. [40].

Owing to its relatively large porosity, and particularly microporosity, porous BN was tested for CO_2 capture under ambient conditions. The results are presented in **Fig. 12**. The capacity measured at 1 bar and 25 °C was about 0.6 mmol/g. It is recognized that this value remains somewhat small when compared to the best CO_2 adsorbents like metal-organic frameworks but it represents a noticeable improvement compared to the reported data in previously published work on CO_2 adsorption using BN-based materials. Indeed, the latter (and few) studies either used different testing conditions that are not relevant to CO_2 capture (e.g. lower temperatures) [4, 5], or reported a lower capacity when tested under the same conditions [6]. Since N_2 is another major component of the flue gas, the material was tested for N_2 adsorption under the same conditions (1 bar, 25 °C) using a gravimetric technique and no uptake was measured indicating promising selectivity.

4. CONCLUSIONS

To conclude, we have performed an in-depth investigation of the effect of synthesis conditions on the formation of porous boron nitride using a bottom-up approach. In particular, it was found that the preparation of the intermediate had a significant impact on the porosity of the resulting boron nitride. Depending on the drying time of that intermediate, the porosity could be more than doubled (from ~400 to 1,000 m^2/g) with a similar increase in microporosity. This dramatic change was assigned to the variation in the thermal decomposition patterns of the intermediates, which in turn led to the formation of an amorphous BN precursor at 250 °C, in different quantities. The intermediates dried for

longer time started decomposing at lower temperatures, which generated the release of gases that acted as porogen during the formation of porous boron nitride. Preliminary CO_2 adsorption tests under ambient condition were run and indicated noticeable capture and good selectivity (compared to N_2). Overall, this study highlights and describes how a synthesis parameter - i.e. precursor preparation - can be used to carefully tune the porosity of boron nitride. Doing this, it provides a piece of the puzzle with regards to the formation of porous boron nitride and offers avenues to design better adsorbents and drug-delivery carriers.

ACKNOWLEDGMENTS

The authors would like to acknowledge the funding from EPSRC through the CDT in Advanced Characterization of Materials as well as the funding and technical support from BP through the BP International Centre for Advanced Materials (BP-ICAM). The authors thank Dr Leslie Bolton and Dr Philip Howard for their technical input. The authors are also grateful to Hannah Leese for her assistance in the TGA-MS measurements.

REFERENCES

[1] X.-F. Jiang, Q. Weng, X.-B. Wang, X. Li, J. Zhang, D. Golberg, Y. Bando, Recent Progress on Fabrications and Applications of Boron Nitride Nanomaterials: A Review, Journal of Materials Science & Technology, (2015).
[2] Y. Lin, J.W. Connell, Advances in 2D boron nitride nanostructures: nanosheets, nanoribbons, nanomeshes, and hybrids with graphene, Nanoscale, 4 (2012) 6908-6939.
[3] F. Xiao, Z. Chen, G. Casillas, C. Richardson, H. Li, Z. Huang, Controllable synthesis of few-layered and hierarchically porous boron nitride nanosheets, Chemical Communications, (2016).

[4] J.F. Janik, W.C. Ackerman, R.T. Paine, D.-W. Hua, A. Maskara, D.M. Smith, Boron nitride as a selective gas adsorbent, Langmuir, 10 (1994) 514-518.
[5] A. Nag, K. Raidongia, K.P. Hembram, R. Datta, U.V. Waghmare, C. Rao, Graphene analogues of BN: novel synthesis and properties, ACS nano, 4 (2010) 1539-1544.
[6] F. Xiao, Z. Chen, G. Casillas, C. Richardson, H. Li, Z. Huang, Controllable synthesis of few-layered and hierarchically porous boron nitride nanosheets, Chemical Communications, 52 (2016) 3911-3914.
[7] J. Li, J. Lin, X. Xu, X. Zhang, Y. Xue, J. Mi, Z. Mo, Y. Fan, L. Hu, X. Yang, Porous boron nitride with a high surface area: hydrogen storage and water treatment, Nanotechnology, 24 (2013) 155603.
[8] Q. Weng, X. Wang, C. Zhi, Y. Bando, D. Golberg, Boron nitride porous microbelts for hydrogen storage, ACS nano, 7 (2013) 1558-1565.
[9] W. Lei, H. Zhang, Y. Wu, B. Zhang, D. Liu, S. Qin, Z. Liu, L. Liu, Y. Ma, Y. Chen, Oxygen-doped boron nitride nanosheets with excellent performance in hydrogen storage, Nano Energy, 6 (2014) 219-224.
[10] M. Maleki, A. Beitollahi, M. Shokouhimehr, Simple Synthesis of Two-Dimensional Micro/Mesoporous Boron Nitride, European Journal of Inorganic Chemistry, (2015).
[11] J. Li, H. Jia, Y. Ding, H. Luo, S. Abbas, Z. Liu, L. Hu, C. Tang, NaOH-embedded three-dimensional porous boron nitride for efficient formaldehyde removal, Nanotechnology, 26 (2015) 475704.
[12] J. Li, X. Xiao, X. Xu, J. Lin, Y. Huang, Y. Xue, P. Jin, J. Zou, C. Tang, Activated boron nitride as an effective adsorbent for metal ions and organic pollutants, Scientific reports, 3 (2013).
[13] X. Zhang, G. Lian, S. Zhang, D. Cui, Q. Wang, Boron nitride nanocarpets: controllable synthesis and their adsorption performance to organic pollutants, CrystEngComm, 14 (2012) 4670-4676.
[14] W. Lei, D. Liu, Y. Chen, Highly Crumpled Boron Nitride Nanosheets as Adsorbents: Scalable Solvent-Less Production, Advanced Materials Interfaces, (2015).
[15] W. Lei, D. Portehault, D. Liu, S. Qin, Y. Chen, Porous boron nitride nanosheets for effective water cleaning, Nature communications, 4 (2013) 1777.
[16] M. Fu, H. Xing, X. Chen, F. Chen, C.-M.L. Wu, R. Zhao, C. Cheng, Ultrathin-shell boron nitride hollow spheres as sorbent for dispersive solid-phase extraction of polychlorinated biphenyls from environmental water samples, Journal of Chromatography A, 1369 (2014) 181-185.
[17] P. Singla, N. Goel, S. Singhal, Boron nitride nanomaterials with different morphologies: Synthesis, characterization and efficient application in dye adsorption, Ceramics International, (2015).
[18] P. Dai, Y. Xue, X. Wang, Q. Weng, C. Zhang, X. Jiang, D. Tang, X. Wang, N. Kawamoto, Y. Ide, Pollutant capturing SERS substrate: porous boron nitride microfibers with uniform silver nanoparticle decoration, Nanoscale, 7 (2015) 18992-18997.
[19] D. Liu, W. Lei, S. Qin, K.D. Klika, Y. Chen, Superior adsorption of pharmaceutical molecules by highly porous BN nanosheets, Physical Chemistry Chemical Physics, 18 (2016) 84-88.

[20] J. Lin, L. Xu, Y. Huang, J. Li, W. Wang, C. Feng, Z. Liu, X. Xu, J. Zou, C. Tang, Ultrafine porous boron nitride nanofibers synthesized via a freeze-drying and pyrolysis process and their adsorption properties, RSC Advances, 6 (2016) 1253-1259.
[21] Y. Xue, P. Dai, X. Jiang, X. Wang, C. Zhang, D. Tang, Q. Weng, X. Wang, A. Pakdel, C. Tang, Template-free synthesis of boron nitride foam-like porous monoliths and their high-end applications in water purification, Journal of Materials Chemistry A, (2016).
[22] H. Zhao, X. Song, H. Zeng, 3D white graphene foam scavengers: vesicant-assisted foaming boosts the gram-level yield and forms hierarchical pores for superstrong pollutant removal applications, NPG Asia Materials, 7 (2015) e168.
[23] X. Wang, C. Zhi, L. Li, H. Zeng, C. Li, M. Mitome, D. Golberg, Y. Bando, "Chemical Blowing" of Thin-Walled Bubbles: High-Throughput Fabrication of Large-Area, Few-Layered BN and Cx-BN Nanosheets, Advanced Materials, 23 (2011) 4072-4076.
[24] X. Wang, A. Pakdel, C. Zhi, K. Watanabe, T. Sekiguchi, D. Golberg, Y. Bando, High-yield boron nitride nanosheets from 'chemical blowing': towards practical applications in polymer composites, Journal of Physics: Condensed Matter, 24 (2012) 314205.
[25] P. Dibandjo, F. Chassagneux, L. Bois, C. Sigala, P. Miele, Comparison between SBA-15 silica and CMK-3 carbon nanocasting for mesoporous boron nitride synthesis, Journal of Materials Chemistry, 15 (2005) 1917-1923.
[26] B. Rushton, R. Mokaya, Mesoporous boron nitride and boron-nitride-carbon materials from mesoporous silica templates, Journal of Materials Chemistry, 18 (2008) 235-241.
[27] S. Schlienger, J. Alauzun, F. Michaux, L. Vidal, J. Parmentier, C. Gervais, F. Babonneau, S. Bernard, P. Miele, J. Parra, Micro-, mesoporous boron nitride-based materials templated from zeolites, Chemistry of Materials, 24 (2011) 88-96.
[28] P. Dibandjo, L. Bois, F. Chassagneux, P. Miele, Thermal stability of mesoporous boron nitride templated with a cationic surfactant, Journal of the European Ceramic Society, 27 (2007) 313-317.
[29] T. O'Connor, Synthesis of boron nitride, Journal of the American Chemical Society, 84 (1962) 1753-1754.
[30] J. Thomas, N. Weston, T. O'connor, Turbostratic1 Boron Nitride, Thermal Transformation to Ordered-layer-lattice Boron Nitride, Journal of the American Chemical Society, 84 (1962) 4619-4622.
[31] T. Hagia, K. Kobayashi, T. Sato, Formation of Hexagonal BN by Thermal Decomposition of Melamine Diborate, Journal of the Ceramic Society of Japan, 102 (1994) 1051-1054.
[32] R. Gao, L. Yin, C. Wang, Y. Qi, N. Lun, L. Zhang, Y.-X. Liu, L. Kang, X. Wang, High-yield synthesis of boron nitride nanosheets with strong ultraviolet cathodoluminescence emission, The Journal of Physical Chemistry C, 113 (2009) 15160-15165.
[33] P. Wu, W. Zhu, Y. Chao, J. Zhang, P. Zhang, H. Zhu, C. Li, Z. Chen, H. Li, S. Dai, A template-free solvent-mediated synthesis of high surface area boron nitride nanosheets for aerobic oxidative desulfurization, Chemical Communications, (2016).
[34] R. Geick, C. Perry, G. Rupprecht, Normal modes in hexagonal boron nitride, Physical Review, 146 (1966) 543.

[35] V. Cholet, L. Vandenbulcke, J. Rouan, P. Baillif, R. Erre, Characterization of boron nitride films deposited from BCl3-NH3-H2 mixtures in chemical vapour infiltration conditions, Journal of materials science, 29 (1994) 1417-1435.
[36] G. Ciofani, G.G. Genchi, I. Liakos, A. Athanassiou, D. Dinucci, F. Chiellini, V. Mattoli, A simple approach to covalent functionalization of boron nitride nanotubes, Journal of colloid and interface science, 374 (2012) 308-314.
[37] A.S. Nazarov, V.N. Demin, E.D. Grayfer, A.I. Bulavchenko, A.T. Arymbaeva, H.J. Shin, J.Y. Choi, V.E. Fedorov, Functionalization and Dispersion of Hexagonal Boron Nitride (h-BN) Nanosheets Treated with Inorganic Reagents, Chemistry–An Asian Journal, 7 (2012) 554-560.
[38] K. Park, D. Lee, K. Kim, D. Moon, Observation of a hexagonal BN surface layer on the cubic BN film grown by dual ion beam sputter deposition, Applied physics letters, 70 (1997) 315-317.
[39] J. Riviere, Y. Pacaud, M. Cahoreau, Spectroscopic studies of BN films deposited by dynamic ion mixing, Thin Solid Films, 227 (1993) 44-53.
[40] X. Gouin, P. Grange, L. Bois, P. L'Haridon, Y. Laurent, Characterization of the nitridation process of boric acid, Journal of alloys and compounds, 224 (1995) 22-28.
[41] O.O. Kurakevych, V.L. Solozhenko, Rhombohedral boron subnitride, B13N2, by X-ray powder diffraction, Acta Crystallographica Section C: Crystal Structure Communications, 63 (2007) i80-i82.
[42] O. Makoto, K. Nobuyoshi, Effect of grinding on the crystallinity and chemical stability in the solid state of cephalothin sodium, International Journal of Pharmaceutics, 62 (1990) 65-73.
[43] J. Worsham, H. Levy, S. Peterson, The positions of hydrogen atoms in urea by neutron diffraction, Acta Crystallographica, 10 (1957) 319-323.
[44] R.R. Shuvalov, P.C. Burns, A new polytype of orthoboric acid, H3BO3-3T, Acta Crystallographica Section C: Crystal Structure Communications, 59 (2003) 47-49.

LIST OF TABLES

Table 1. BET equivalent surface area, total volume of pores, volume of micropores and volume of mesopores of the different porous boron nitride samples, as measured using N_2 sorption at -196 °C. The table also report the d-spacing derived from the XRD patterns for the different BN samples.

Sample	S_{BET} (m^2/g)	V_{tot} (cm^3/g)	V_{mic} (cm^3/g)	V_{mes} (cm^3/g)	V_{mic}/V_{tot}	$d_{(002)}$ (Å)
BN-0	403	0.625	0.164	0.461	0.262	3.51
BN-50	514	0.654	0.212	0.442	0.324	3.54
BN-100	695	0.719	0.273	0.446	0.380	3.56
BN-200	1016	0.869	0.417	0.452	0.480	3.60
BN-phys mix	945	0.852	0.389	0.463	0.457	3.60

FIGURES CAPTIONS

Figure 1. FTIR spectra of porous BN samples. The materials were obtained from intermediates prepared by recristallyzing urea and boric acid from water and drying them for varying durations.

Figure 2. XPS core level spectra of the porous BN sample. The materials was derived from a physical mixture between urea and boric acid (BN-phys mix sample), together with the relative atomic percentages for B 1*s*, N 1*s* and O 1*s* for the different porous BN samples derived from XPS analysis.

Figure 3. XRD patterns of porous BN samples. The materials were synthesized from the various intermediates. The dotted lines correspond to reference values for h-BN from [41].

Figure 4. N_2 sorption isotherms for the porous BN samples. The materials were synthesized from different intermediates and the isotherms were measured at -196 ^{o}C.

Figure 5. High-resolution SEM images of porous BN. The sample is BN-0 and exhibits the two main macroscale features of the material: (left) flakes and (right) macropores.

Figure 6. Typical high resolution TEM images of porous BN. The sample is BN-0.

Figure 7. XPS core level spectra of intermediates used to synthesize porous BN. These samples include: he physical mixture of urea and boric acid as well as the intermediate samples INT-0 and INT-200. The spectra were normalized to the O 1s peak.

Figure 8. XRD patterns of the precursors and intermediates used to synthesize porous BN. The dotted lines represent values from reference patterns for urea [43] and boric acid [44].

Figure 9. Thermal analyses of the precursors and intermediates used to synthesize porous BN. The curves represent the thermogravimetric (TG) curves and were obtained under N_2 atmosphere.

Figure 10. Overview of the species released during porous BN formation. The panels represent the mass spectra for ammonia, carbon dioxide, cyanic acid and water vapor released during decomposition under N_2 atmosphere of the intermediates and the physical mixture of boric acid and urea.

Figure 11. XPS spectra before and after heat treatment of an intermediate as well as porous BN. The intermediate sample is INT-0. The porous BN sample is BN-0. INT-0 was

analysed before and after heat treatment at 250 °C. BN-0 was synthesized using INT-0 and heating it at 1050 °C under nitrogen gas flow.

Figure 12. CO_2 capture using porous BN. CO_2 sorption isotherm measured at 25 °C and up to the pressure of 1 bar of BN produced from an intermediate dried for 200 h.

LIST OF FIGURES

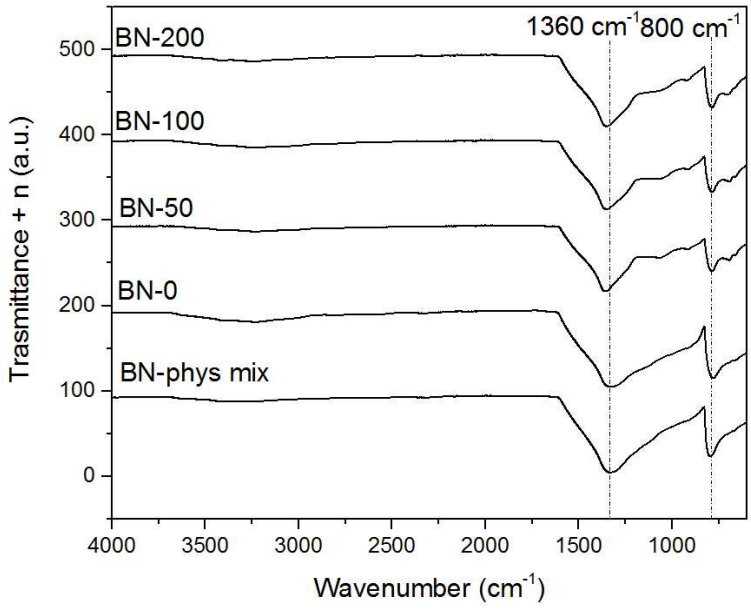

Figure 1. FTIR spectra of porous BN samples. The materials were obtained from intermediates prepared by recristallyzing urea and boric acid from water and drying them for varying durations.

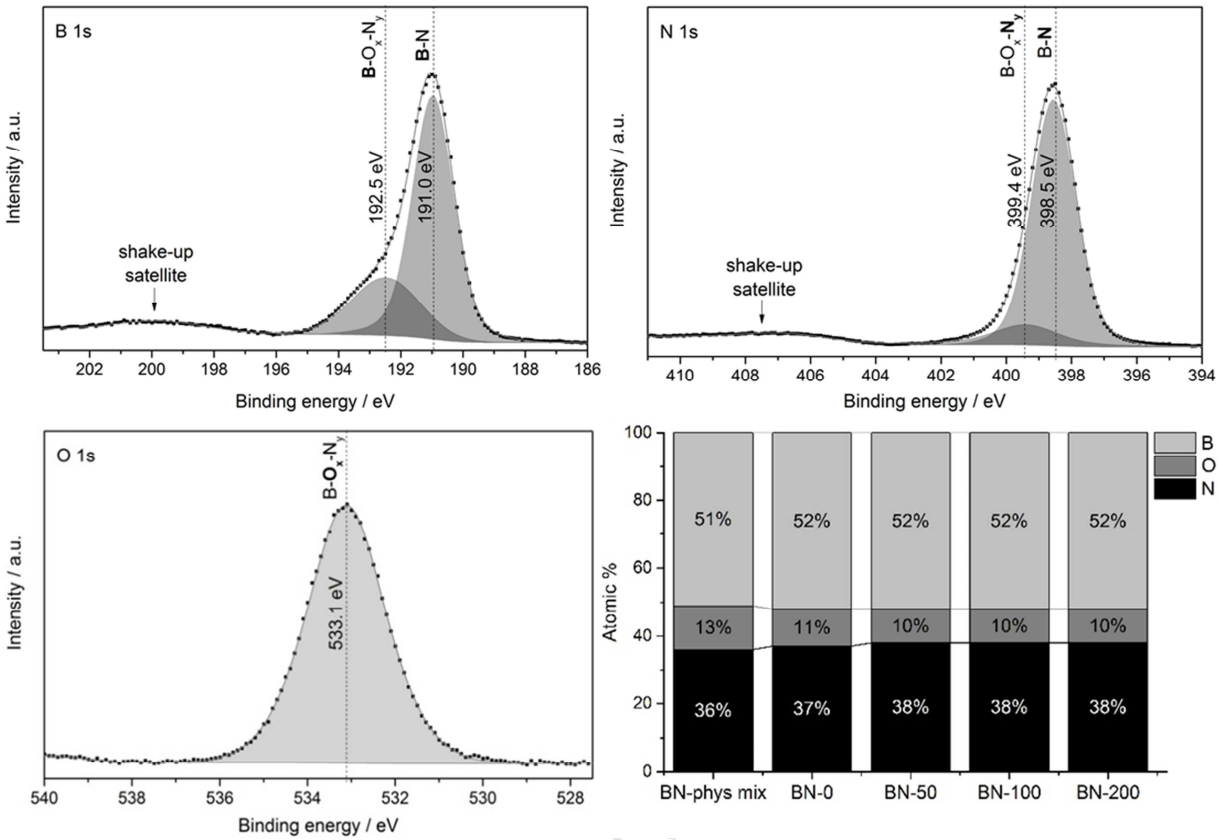

Figure 2. XPS core level spectra of the porous BN sample. The material was derived from a physical mixture between urea and boric acid (BN-phys mix sample), together with the relative atomic percentages for B 1*s*, N 1*s* and O 1*s* for the different porous BN samples derived from XPS analysis.

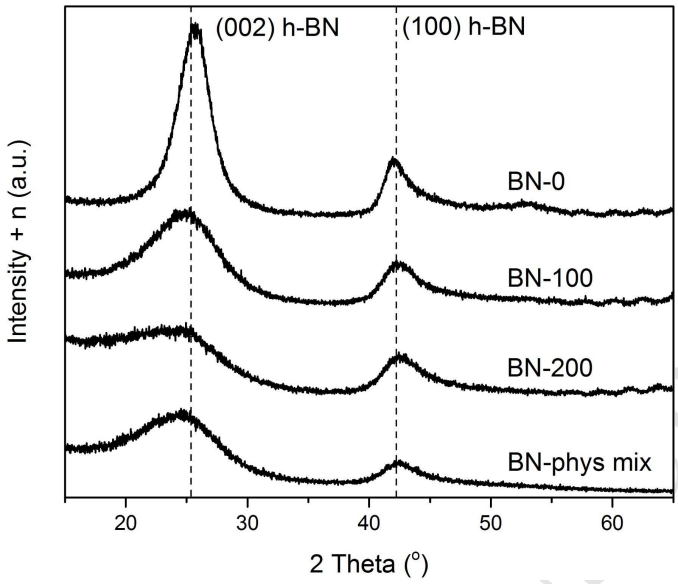

Figure 3. XRD patterns of porous BN samples. The materials were synthesized from the various intermediates. The dotted lines correspond to reference values for h-BN from [41].

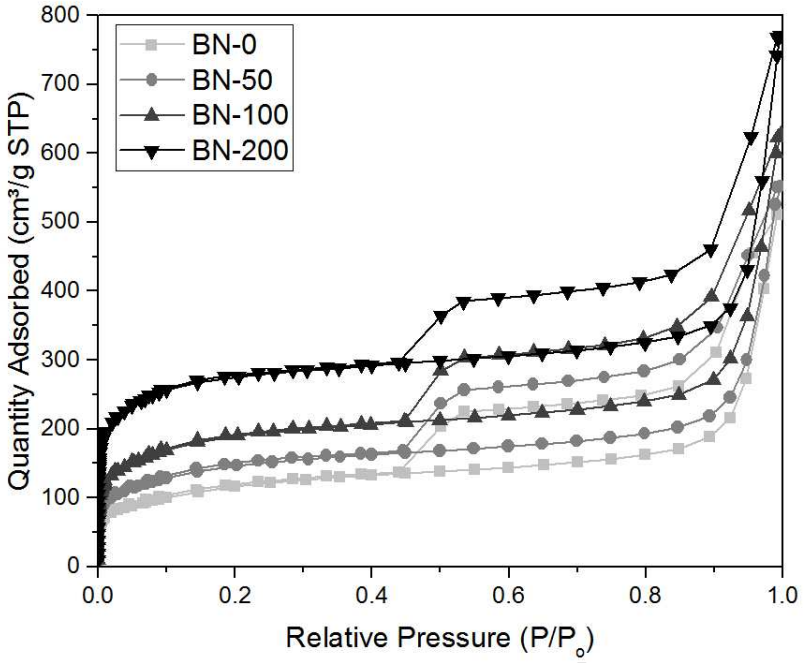

Figure 4. N_2 sorption isotherms for the porous BN samples. The materials were synthesized from different intermediates and the isotherms were measured at -196 ^{o}C.

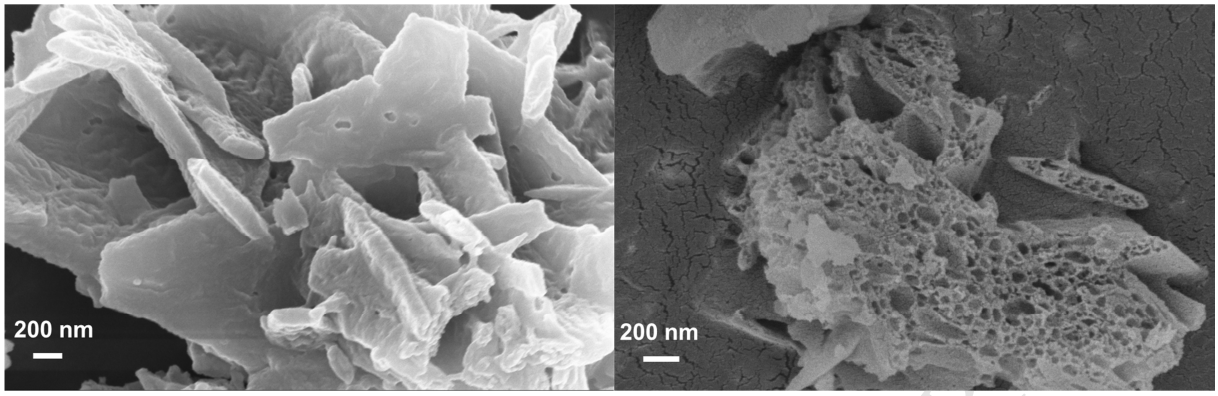

Figure 5. High-resolution SEM images of porous BN. The sample is BN-0 and exhibits the two main macroscale features of the material: (left) flakes and (right) macropores.

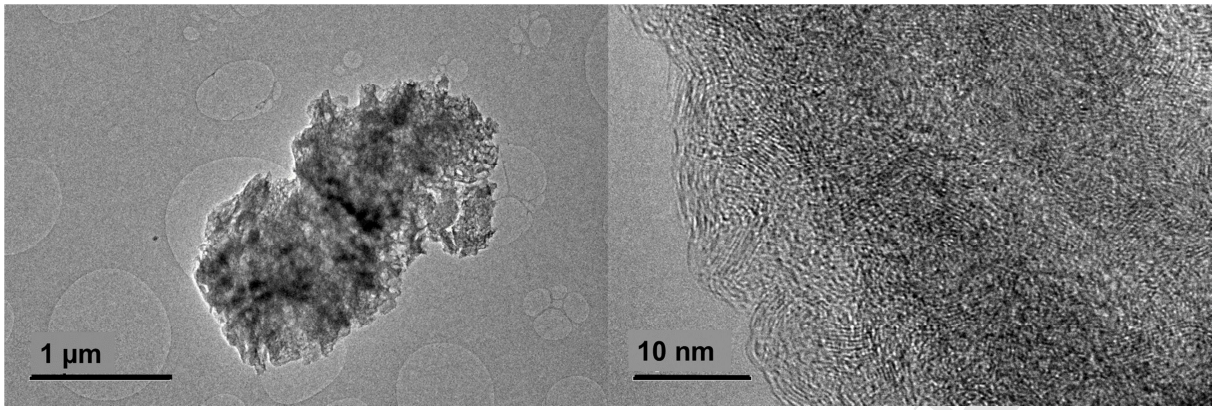

Figure 6. Typical high resolution TEM images of porous BN. The sample is BN-0.

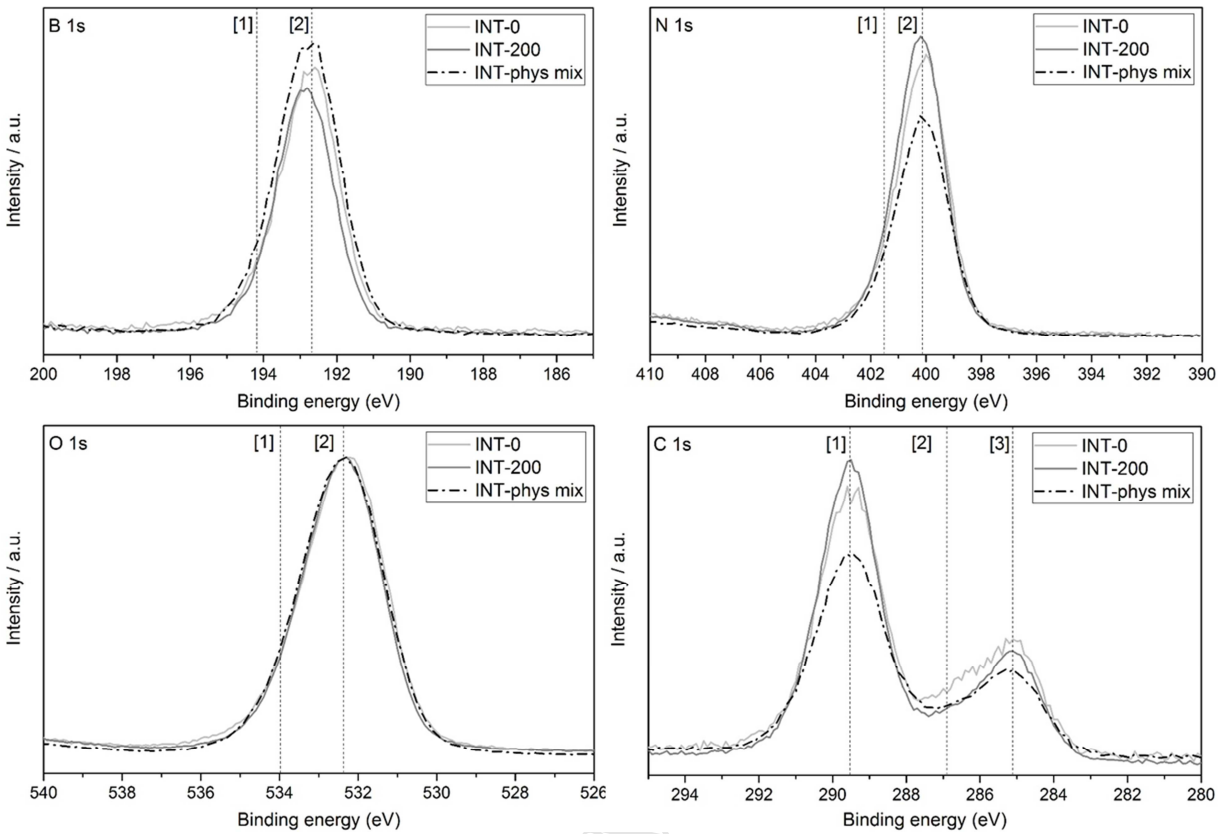

Figure 7. XPS core level spectra of intermediates used to synthesize porous BN. These intermediates include: the physical mixture of urea and boric acid as well as the intermediate samples INT-0 and INT-200. The spectra were normalized to the O 1s peak.

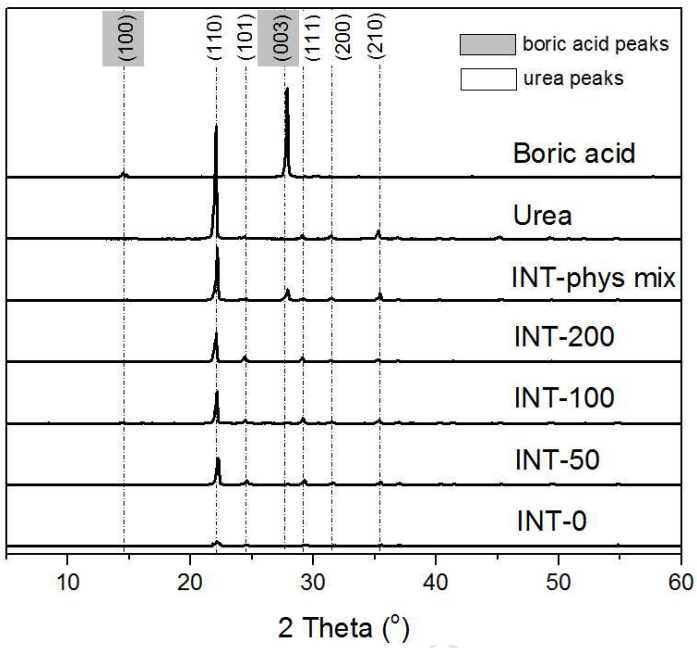

Figure 8. XRD patterns of the precursors and intermediates used to synthesize porous BN.

The dotted lines represent values from reference patterns for urea [43] and boric acid [44].

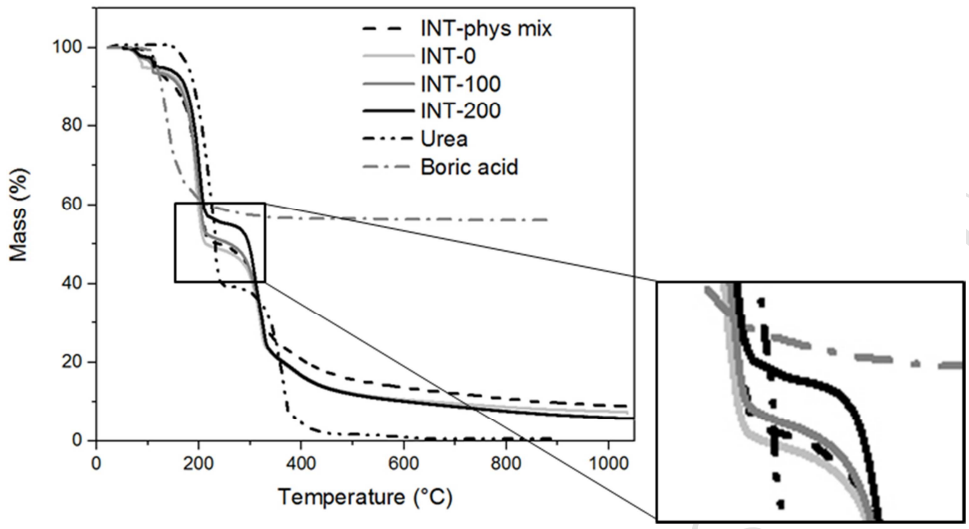

Figure 9. Thermal analyses of the precursors and intermediates used to synthesize porous BN. The curves represent the thermogravimetric (TG) curves and were obtained under N_2 atmosphere.

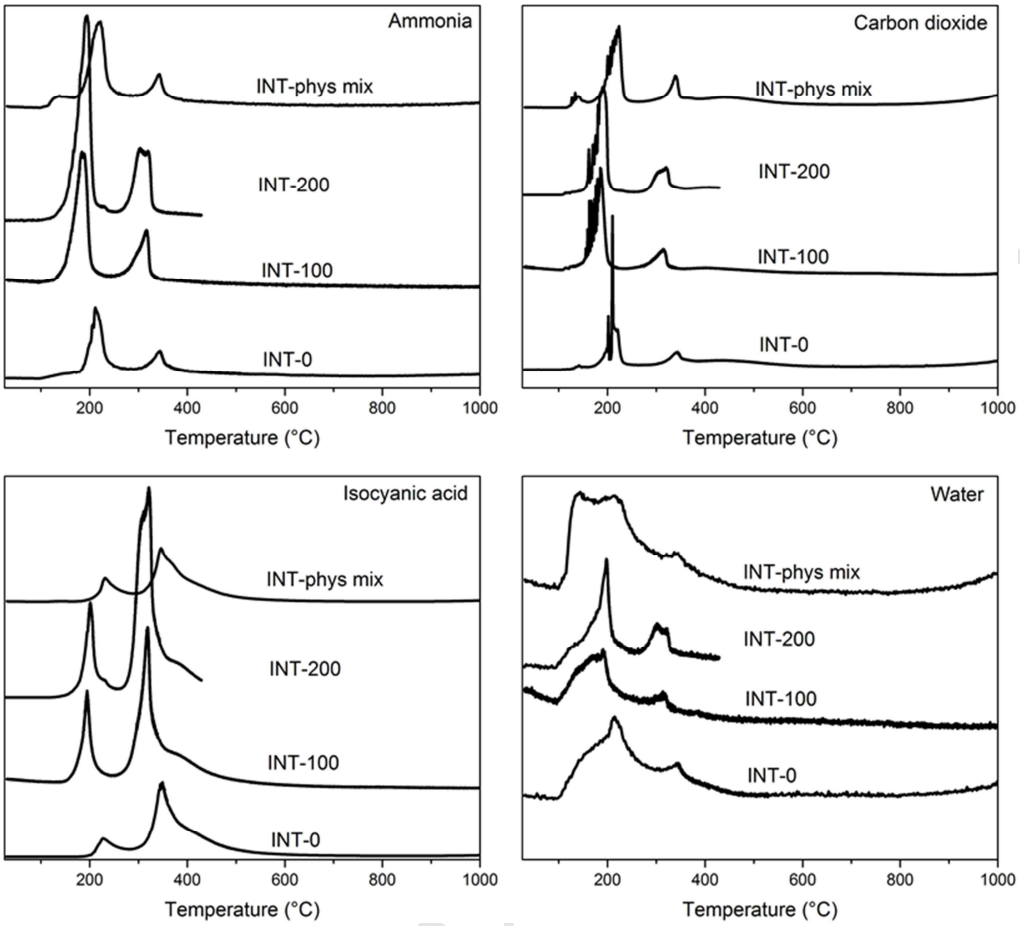

Figure 10. Overview of the species released during porous BN formation. The panels represent the mass spectra for ammonia, carbon dioxide, cyanic acid and water vapor released during decomposition under N_2 atmosphere of the intermediates and the physical mixture of boric acid and urea.

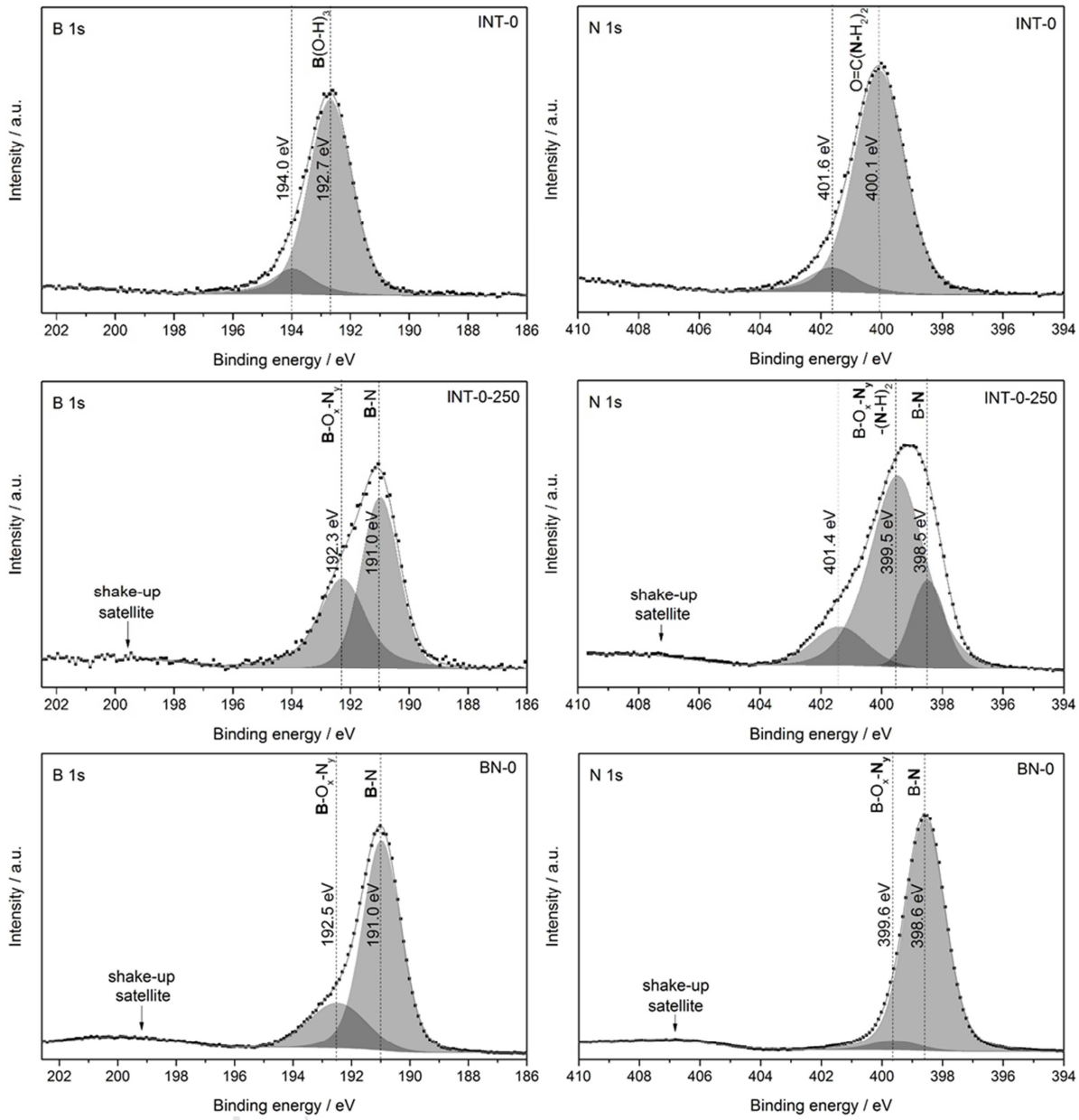

Figure 11. XPS spectra before (top) and after (middle) heat treatment of an intermediate as well as porous BN (bottom). The intermediate sample is INT-0. The porous BN sample is BN-0. INT-0 was analysed before and after heat treatment at 250 °C. BN-0 was synthesized using INT-0 and heating it at 1050 °C under nitrogen gas flow.

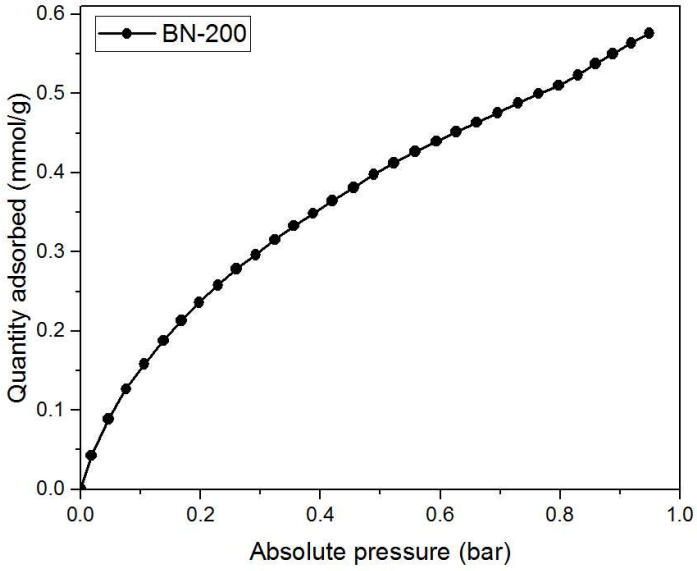

Figure 12. CO_2 capture using porous BN. CO_2 sorption isotherm measured at 25 °C and up to the pressure of 1 bar of BN produced from an intermediate dried for 200 h.

Tunable porous boron nitride: investigating its formation and its application for gas adsorption

Sofia Marchesini,[a] *Anna Regoutz,*[b] *David Payne*[b] *and Camille Petit*[a,*]

[a] Department of Chemical Engineering, Imperial College London, South Kensington Campus, London SW7 2AZ, UK

[b] Department of Materials, Imperial College London, South Kensington Campus, London SW7 2AZ, UK

Highlights

- The porosity of boron nitride (BN) is tuned by controlling its intermediate formation
- Porosity is tailored is via the intermediates varying thermal decomposition patterns
- Highly porous BN is obtained (>1,000 m^2/g) with both mesopores and micropores
- As produced porous BN exhibit good adsorption selectivity of CO_2 over N_2

* Corresponding Author: Camille Petit, camille.petit@imperial.ac.uk